Science of the Total Environment 765 (2021) 144338

Contents lists available at ScienceDirect

Science of the Total Environment

journal homepage: www.elsevier.com/locate/scitotenv

Role of emission controls in reducing the 2050 climate change penalty for $PM_{2.5}$ in China

Song Liu [a,b], Jia Xing [a,b,*], Daniel M. Westervelt [c,d], Shuchang Liu [a,b], Dian Ding [a,b], Arlene M. Fiore [c,e], Patrick L. Kinney [f], Yuqiang Zhang [g], Mike Z. He [h], Hongliang Zhang [i], Shovan K. Sahu [a,b], Fenfen Zhang [a,b], Bin Zhao [j], Shuxiao Wang [a,b,*]

[a] State Key Joint Laboratory of Environmental Simulation and Pollution Control, School of Environment, Tsinghua University, Beijing, China
[b] State Environmental Protection Key Laboratory of Sources and Control of Air Pollution Complex, Beijing, China
[c] Lamont-Doherty Earth Observatory, Columbia University, Palisades, New York, NY, USA
[d] NASA Goddard Institute for Space Studies, New York, NY, USA
[e] Department of Earth and Environmental Sciences, Columbia University, Palisades, New York, NY, USA
[f] School of Public Health, Boston University, Boston, MA, USA
[g] Nicholas School of the Environment, Duke University, Durham, NC, USA
[h] Department of Environmental Health Sciences, Columbia University Mailman School of Public Health, New York, NY, USA
[i] Department of Environmental Science and Engineering, Fudan University, Shanghai, China
[j] Pacific Northwest National Laboratory, Richland, WA, USA

HIGHLIGHTS

- Future climate under RCP8.5 will increase $PM_{2.5}$ by over 1 μg m^{-3} in Eastern China.
- 14% of $PM_{2.5}$ decrease from emission controls occurs by reducing climate penalty.
- Over one-third of $PM_{2.5}$-mortality can be avoided after strict emission reductions.

GRAPHICAL ABSTRACT

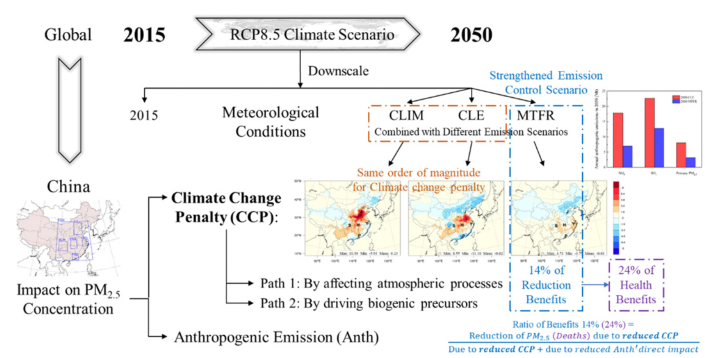

ARTICLE INFO

Article history:
Received 30 September 2020
Received in revised form 2 December 2020
Accepted 3 December 2020
Available online 25 December 2020

Editor: Jianmin Chen

Keywords:
Downscaling
Emission scenarios
Climate change penalty
$PM_{2.5}$
China

ABSTRACT

Previous studies demonstrated that global warming can lead to deteriorated air quality even when anthropogenic emissions were kept constant, which has been called a climate change penalty on air quality. It is expected that anthropogenic emissions will decrease significantly in the future considering the aggressive emission control actions in China. However, the dependence of climate change penalty on the choice of emission scenario is still uncertain. To fill this gap, we conducted multiple independent model simulations to investigate the response of $PM_{2.5}$ to future (2050) climate warming (RCP8.5) in China but with different emission scenarios, including the constant 2015 emissions, the 2050 CLE emissions (based on Current Legislation), and the 2050 MTFR emissions (based on Maximum Technically Feasible Reduction). For each set of emissions, we estimate climate change penalty as the difference in $PM_{2.5}$ between a pair of simulations with either 2015 or 2050 meteorology. Under 2015 emissions, we find a $PM_{2.5}$ climate change penalty of 1.43 μg m^{-3} in Eastern China, leading to an additional 35,000 $PM_{2.5}$-related premature deaths [95% confidence interval (CI), 21,000-40,000] by 2050. However, the $PM_{2.5}$ climate change penalty weakens to 0.24 μg m^{-3} with strict anthropogenic emission controls under the 2050 MTFR emissions, which decreases the associated $PM_{2.5}$-related deaths to 17,000. The smaller MTFR climate

* Corresponding authors at: State Key Joint Laboratory of Environmental Simulation and Pollution Control, School of Environment, Tsinghua University, Beijing, China.
E-mail addresses: xingjia@tsinghua.edu.cn (J. Xing), shxwang@tsinghua.edu.cn (S. Wang).

https://doi.org/10.1016/j.scitotenv.2020.144338

change penalty contributes 14% of the total $PM_{2.5}$ decrease when both emissions and meteorology are changed from 2015 to 2050, and 24% of total health benefits associated with this $PM_{2.5}$ decrease in Eastern China. This finding suggests that controlling anthropogenic emissions can effectively reduce the climate change penalty on $PM_{2.5}$ and its associated premature deaths, even though a climate change penalty still occurs even under MTFR. Strengthened controls on anthropogenic emissions are key to attaining air quality targets and protecting human health in the context of future global climate change.

1. Introduction

It is estimated that the human exposure to ambient $PM_{2.5}$ (Particulate Matter with an aerodynamic equivalent diameter of less than 2.5 μm) has led to 3.7–4.8 million global deaths and 1.1–1.3 million deaths in China in 2015 (Cohen et al., 2017). To protect human health, the China government implemented the "Air Pollution Prevention and Control Action Plan" in 2013 (The State Council of the People's Republic of China, 2013) and effectively reduced the $PM_{2.5}$ concentrations in the key regions such as Beijing-Tianjin-Hebei region (also called the Jing-Jin-Ji region or JJJ) and the Yangtze River Delta (YRD) (Ding et al., 2019). However, heavy pollution events still frequently occur (Li, 2019) and $PM_{2.5}$ concentrations in most Chinese cities still far exceed the World Health Organization (WHO) recommended values (<10 μg m^{-3}).

In addition to the needs for continuously strengthened controls on anthropogenic air pollutant emissions, another important challenge is the "climate change penalty", which is defined as the deterioration of air quality due to a warming climate in the absence of changes in anthropogenic polluting activities (Fu and Tian, 2019; Jacob and Winner, 2009). Previous studies have demonstrated that the climate change penalty will play an important role in determining future $PM_{2.5}$ concentrations (Gao et al., 2019; Heald et al., 2008; Liao et al., 2006; Liu et al., 2017; Westervelt et al., 2016; Yin et al., 2015; Zhang et al., 2018). For example, Jiang et al. (2013) estimated that $PM_{2.5}$ concentration will increase by 10–20% due to climate change penalty in eastern China from 2000 to 2050 using GEOS-Chem model under the IPCC A1B scenario. Leung et al. (2017) suggested that climate change under the Representative Concentration Pathway 8.5 (RCP8.5) scenario could be responsible for increases in $PM_{2.5}$ of more than 25 μg m^{-3} in northwestern China and 10 μg m^{-3} in northeastern China by the 2050s using a forward-selection multiple linear regression (MLR) model. Climate change also influences air quality by affecting biogenic emissions (Liu et al., 2019b; Xie et al., 2017). For example, Heald et al. (2008) suggested that biogenic emissions will increase by around 20% under the IPCC A1B scenario, resulting in an increased global mean secondary organic aerosols (SOA) by 26% in 2100 using the Community Atmosphere Model (CAM3) and the Model of Emissions of Gases and Aerosols from Nature (MEGAN). Jiang et al. (2010) found that increasing isoprene emissions become the major contributor to SOA formation over Texas in the 2050s under the A1B scenario.

However, future mitigation of CO_2 and other greenhouse gases (GHGs) suffers large uncertainties especially after the U.S. withdrawal from the Paris Agreement in 2019 (Su and Teng, 2019). The climate change penalty seems unavoidable as emission rates of CO_2 and other GHGs continue to rise. It is important to understand how the climate change penalty would be if we just control the anthropogenic emissions associated with air pollution under a warming future scenario.

To address the concern above, in this study we investigate how the climate penalty for $PM_{2.5}$ under RCP8.5 varies across different air pollution emission pathways in China. The remainder of this paper is organized as follows: Section 2 describes research methods; Section 3.1 introduces the future meteorological condition and biogenic emissions; Section 3.2 discusses the climate change penalty and its affecting mechanism based on different emissions; Section 3.3 introduces the benefits in air quality and health caused by climate change penalty due to emission reduction. The summary and conclusion are given in Section 4.

2. Method

2.1. Global climate model downscaling and WRF-CMAQ configuration

Based on Climate Data Operators (CDO) (Schulzweida et al., 2006), we re-gridded (e.g. from hybrid to pressure levels) the global meteorological fields simulated by Westervelt et al. (2019) using the Geophysical Fluid Dynamics Laboratory Atmospheric Model version 3 (GFDL-AM3) (Donner et al., 2011; Levy et al., 2013) for dynamical downscaling with the regional Weather Research and Forecasting Model (WRF, version 3.7.1). Meteorological variables considered include temperature, specific humidity, pressure, surface height, wind speed, land mask, ice mask, soil temperature and soil moisture. Global simulations are averaged to dampen climate variability and thus span 10 years for a 2015 climate (average of 2010–2019) as well as for a 2050 climate (average of 2046–2055 to represent 2050). The same sea surface temperatures (SSTs), sea ice cover (SICs) and well-mixed GHGs (under RCP8.5) in 2050 were imposed in all 2050 global simulations. Aerosols and ozone interact with climate through their influences on clouds and radiation in the global simulations. We used the WRF model to simulate regional meteorological fields.

The Community Multiscale Air Quality Model (CMAQ, version 5.2.1) configured with the AERO6 aerosol module (Appel et al., 2013) and the Carbon Bond 6 (CB6) gas-phase chemical mechanism (Sarwar et al., 2008) was used to simulate $PM_{2.5}$ concentrations (Appel et al., 2018; Byun, 1999). MEGAN (version 2.10) (Guenther et al., 2012) was used to calculate emissions of Biogenic Volatile Organic Compounds (BVOC), for which the year-specific leaf area index (LAI) data are from the 8-day Moderate Resolution Imaging Spectroradiometer (MODIS) LAI product (MOD15A2) (Hu et al., 2017). The anthropogenic emissions used in CMAQ will be introduced in Section 2.2. The initial and boundary conditions for CMAQ simulation are derived from the downscaling of the GFDL-AM3 global model. The remapping method of chemical species is detailed in Table S1. The online coupling of lightning, dust, soil emissions and future changes of plant function and land cover types were not considered in this study due to lack of data support. The Meteorology-Chemistry Interface Processor (MCIP, version 4.3) (Otte and Pleim, 2010) was used to process meteorological data in the format required by the MEGAN and CMAQ.

The modeling domain covers East Asia, northern Southeast Asia and northeastern India with a 27 km × 27 km grid resolution. A Lambert projection with the domain origin of 34°N, 110°E and with two true latitudes of 25°N and 40°N was used (Zhao et al., 2013). The simulation of the meteorological field uses 35 vertical layers, and the chemical field uses 14 layers (from ground to 100 hPa). Concentrations in ground layer were used for analysis. The simulation period for CMAQ covers the whole year of 2015 and 2050. A five-day simulation spin-up was performed in regional simulations to minimize the effects of initial conditions as in previous studies (Ding et al., 2019; Streets et al., 2007; Wang et al., 2012). The region-specific analysis covers five typical regions (Liu et al., 2019b): Beijing-Tianjin-Hebei region (denoted as JJJ), the Yangtze River Delta (denoted as YRD), the Pearl River Delta (denoted as PRD), the Sichuan Basin (denoted as SCH) and central China (denoted as HUZ) as shown in Fig. 1. Eastern China that includes the above five typical regions (denoted as ECH) and Mainland China (denoted as CHA) are used for specific calculations

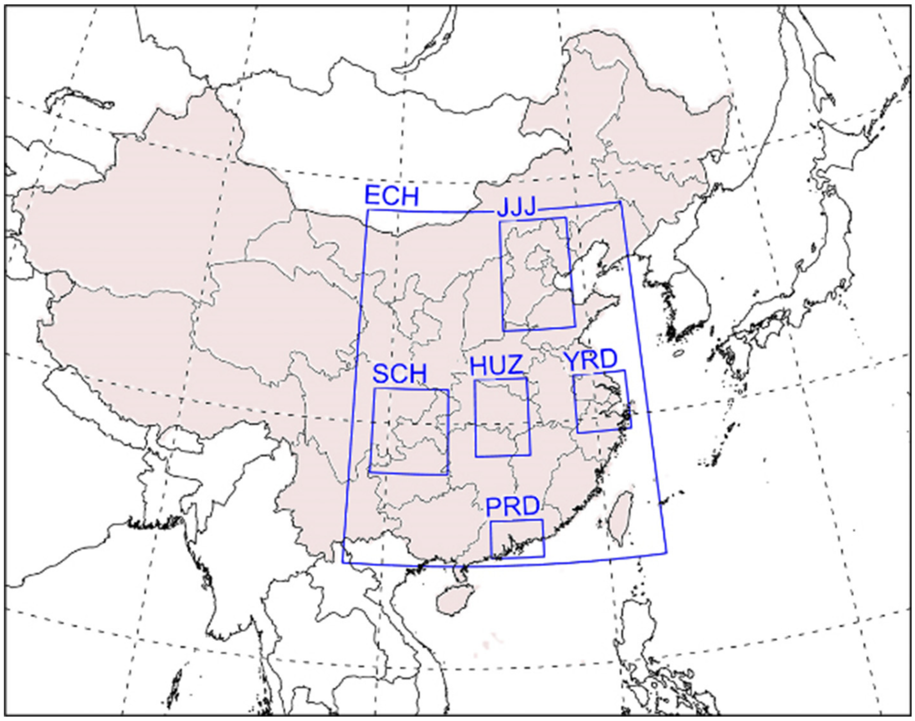

Fig. 1. The modeling domain with a grid resolution of 27 km (182 × 232 cells) and the locations of the five typical regions (i.e., JJJ, YRD, PRD, SCH and HUZ. J, Y, P, S, and H are marked at the center of the regions in the following figures), eastern China (ECH) and mainland China (CHA, shaded part).

to analyze overall trends. The main parameter settings of the WRF-CMAQ model are listed in Table S2.

2.2. Anthropogenic emissions

We prepared three sets of anthropogenic emission inventories for the CMAQ simulations. The anthropogenic emissions inventory for China in 2015 from Air Benefit and Cost and Attainment Assessment System-National Emissions Inventory (AbaCAS-EI) (Zheng et al., 2019) includes the pollutants nitrogen oxides (NO_x), sulfur dioxide (SO_2), PM_{10}, $PM_{2.5}$, organic carbon (OC), black carbon (BC), volatile organic compounds (VOCs), ammonia (NH_3) as detailed by Zhao et al. (2018) and Ding et al. (2019). CO was downscaled based on the inventory named Evaluating the Climate and Air Quality Impacts of Short-Lived Pollutants version5a (ECLIPSE v5a) (Stohl et al., 2015). We included two future emission inventories from International Institute for Applied Systems Analysis (IIASA): Current Legislation (CLE) and Maximum Technically Feasible Reduction (MTFR) from the ECLIPSE v5a dataset to be used for 2050 over China (Stohl et al., 2015). CLE includes current and planned environmental laws, considering known delays and failures up to now but assuming full enforcement in the future. The mitigation basket under the MTFR emission scenario contains three groups of measures: centrally implemented measures that affect emissions of methane (CH_4), technical measures that reduce the emissions of BC, and nontechnical measures to eliminate BC emissions, leading to only minor reductions in CO_2 emissions but large reductions in most short-lived climate pollutants (SLCPs) compared to the CLE emission scenario (Stohl et al., 2015). The gridded ECLIPSE emissions (resolution is $0.5° \times 0.5°$) are re-gridded into 27 km × 27 km to match with the CMAQ model. Chemical species are also remapped to match species in the CB6-AERO6 used in CMAQ based on the methods by Liu et al. (2018).

The national anthropogenic emissions for NO_x, SO_2 and primary $PM_{2.5}$ are 20.44, 14.40 and 7.19 Mt., respectively, in 2015 (calculated as sum of emissions from each province). Distributions of annual emissions of NO_x, SO_2 and primary $PM_{2.5}$ for two 2050 emission scenarios in simulation domain are shown in Fig. 2. Anthropogenic emissions for NO_x, SO_2 and primary $PM_{2.5}$ are 17.85, 22.68 and 8.07 Mt., respectively, in CHA under 2050 CLE emission scenario (calculated as sum of grid values after downscaling). Although the total emissions under the CLE emission scenario are similar with 2015 over CHA, there are still typical regions where emissions tend to increase, such as NO_x emission in YRD and SO_2 emission in JJJ, YRD, and PRD. Due to the different sources of the 2015 and 2050 CLE inventories, we use 2015 to conduct a more realistic simulation for base year, and 2050 CLE for comparison with 2050 MTFR. Compared with 2050 CLE, the annual emissions of the three pollutants in the 2050 MTFR emission scenario will decrease by 61%, 43% and 60%, respectively, as shown in Figs. 2 and S1.

2.3. Health assessment

The $PM_{2.5}$-related mortality in China was computed with U.S. EPA's Benefits Mapping and Analysis Program-Community Edition (BenMAP-CE, version 1.4) model (Voorhees et al., 2014). The results estimated by BenMAP may be lower than the results of the Global Exposure Mortality Model (GEMM) (Burnett et al., 2018), but it is still a widely used tool (Ding et al., 2019; Liu et al., 2019a). We kept the population and baseline mortality rates constant for the future analysis. We applied the Integrated Exposure-Response (IER) model results developed by the Global Burden of Disease (GBD) 2015 study (Cohen et al., 2017) to estimate the disease burden attributable to $PM_{2.5}$. The relative risk model method was used to estimate the health impacts of $PM_{2.5}$ as follows:

$$\Delta Y = Y_0\,(1-1/RR)\,POP$$

where ΔY is an attributable case of health end point related to $PM_{2.5}$ exposure, Y_0 is the baseline incidence rate, *POP* is the total exposed population (for adults above 25), *RR* is the relative risk for the specific health end point, and $(1-1/RR)$ represents the fraction of incidence rates attributable to $PM_{2.5}$ (Fann et al., 2013; Kan and Chen, 2004).

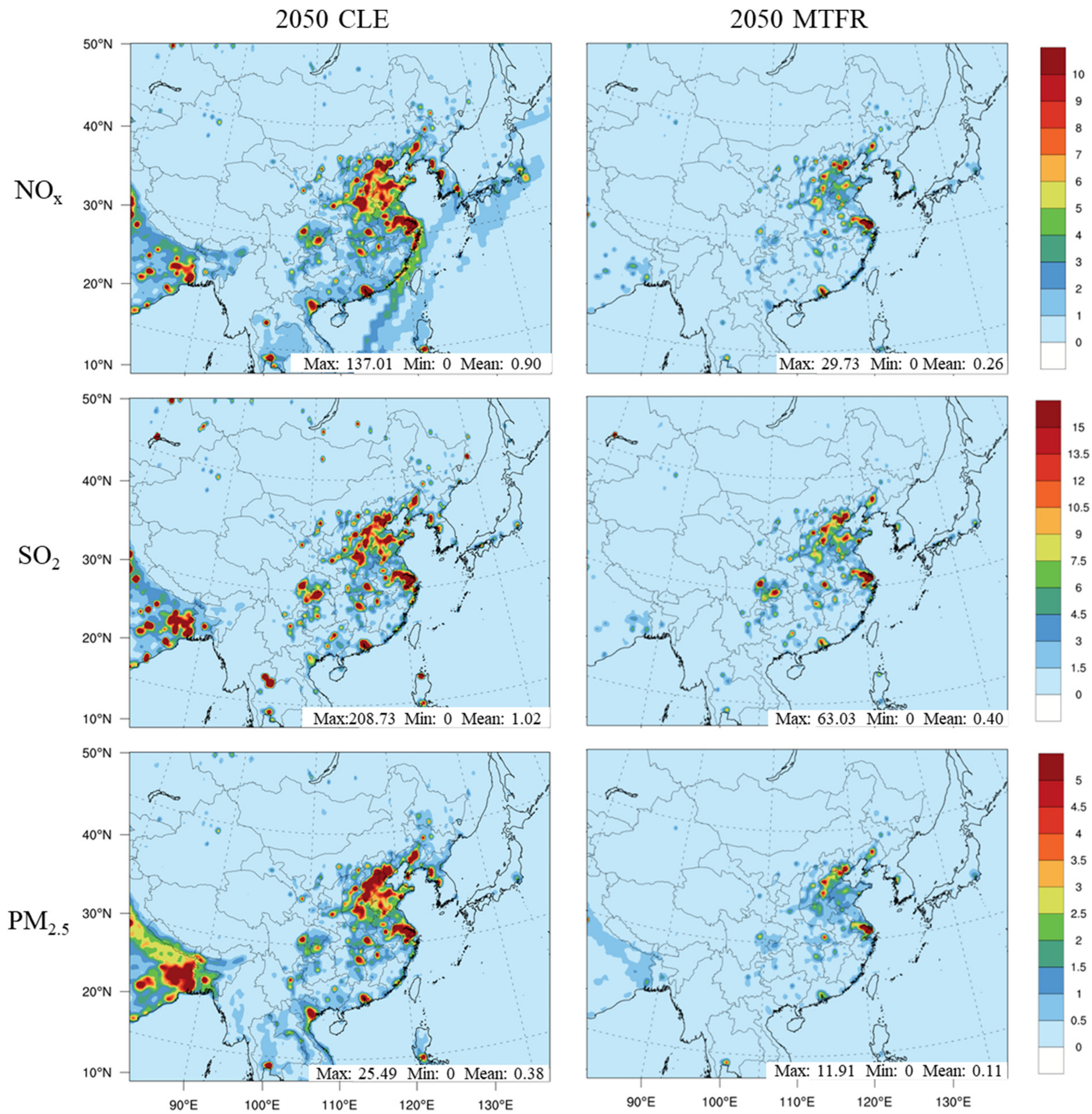

Fig. 2. Distributions of annual emissions of anthropogenic NO_x, SO_2 and primary $PM_{2.5}$ for two 2050 emission scenarios (i.e., 2050 CLE and 2050 MTFR) (Unit: kt).

2.4. Experiment design

We used the RCP8.5 climate scenario sampled for 2015 and 2050 conditions. By using the global GFDL-AM3 model simulations in Westervelt et al. (2019) as boundary conditions for WRF, we downscaled 2015 plus three sets of 2050 meteorology under the same RCP8.5 climate scenario that were combined with different anthropogenic air pollutant emissions: 1) 2015 baseline emission; 2) 2050 ECLIPSEv5a CLE emission and 3) 2050 ECLIPSEv5a MTFR emission scenarios (Stohl et al., 2015). This enables a sensitivity study of the response to climate change with different air pollutant emissions. We use these four downscaled meteorological fields to drive the following ten CMAQ simulations: 1) base year meteorology with base year emission in 2015 (denoted as 2015); 2) CLE meteorology with CLE emission in 2050 (denoted as 2050 CLE); 3) MTFR meteorology with MTFR emission in 2050 (denoted as 2050 MTFR); and 4) CLIM meteorology with 2015 emission (global simulation using 2015 emission with 2050 meteorology, denoted as 2050 CLIM). We ensure that all the 2050 meteorological fields match with their corresponding emissions used in the global GFDL-AM3 climate model simulations, with the aim of achieving consistency between the radiative and cloud feedback effects of different air pollutant emissions on climate in the global GFDL-AM3 simulations with the emissions used in the regional CMAQ simulations. Feedback effects of emissions on climate are not considered in our regional simulations, further the 2015 emissions inventories in the regional CMAQ and global GFDL-AM3 models differ (regional ABaCAS-EI only include China, so ECLIPSEv5a CLE 2015 were used in global models).

By pairing simulations with 2015 and 2050 meteorology but the same emissions for both time periods, we can estimate the climate change penalty (noted as CCP in the following text) for RCP8.5 under three different emission levels, as listed in Table 1. In group 1, CCP using 2015 emissions (CCP_{E2015}) is estimated from the difference between 2050CLIM and 2015BASE. Groups 2 and 3 can estimate CCP using 2050CLE emissions ($CCP_{E2050CLE}$) and 2050 MTRF emissions ($CCP_{E2050MTFR}$) and further separate influence through two CCP mechanisms, respectively (calculation formulas are listed in Table 1). CCP

Table 1
Sensitivity analysis for quantifying the individual impact of each mechanism on $PM_{2.5}$. The abbreviations for standard simulations are listed on the last column.

Group	Case No.	Meteorological fields	Modification	Objective	Notation
1. 2015 Emission	1.1	2015		Base simulation.	2015BASE
	1.2	2050 CLIM	Using 2015 emissions and 2050 CLIM meteorological fields.	CCP_{E2015} = Case 1.2 – Case 1.1	2050CLIM
2. 2050 CLE Emission	2.1	2050 CLE		Standard 2050CLE simulation.	2050CLE
	2.2	2015	Changing meteorological fields and biogenic emissions to 2015.	$CCP_{E2050CLE}$ = Case 2.1 – Case 2.2	
	2.3	2050 CLE	Changing biogenic emissions to 2015.	$CCP_{E2050CLE}$-Bio = Case 2.1 – Case 2.3; $CCP_{E2050CLE}$-Met = Case 2.3 – Case 2.2.	
	2.4	2050 CLE	Changing anthropogenic emissions to 2015.	$\Delta Anth_{E2050CLE}$ = Case 2.1 – Case 2.4.	
3. 2050 MTFR Emission	3.1	2050 MTFR		Standard 2050MTFR simulation.	2050MTFR
	3.2	2015	Changing meteorological fields and biogenic emissions to 2015.	$CCP_{E2050MTFR}$ = Case 3.1 – Case 3.2.	
	3.3	2050 MTFR	Changing biogenic emissions to 2015.	$CCP_{E2050MTFR}$-Bio = Case 3.1 – Case 3.3; $CCP_{E2050MTFR}$-Met = Case 3.3 – Case 3.2.	
	3.4	2050 MTFR	Changing anthropogenic emissions to 2015.	$\Delta Anth_{E2050MTFR}$ = Case 3.1 – Case 3.4.	

All meteorological fields are using RCP8.5 climate scenarios.

mechanisms include the effect of meteorological factors on atmospheric chemical and physical processes including reaction rates, mixing depth, stagnation, wind speed, hygroscopic growth, wet and dry deposition, etc. ($CCP_{E2050CLE/MTFR}$-Met) and by driving biogenic emissions (i.e., pollutant precursors) such as isoprene, monoterpenes, etc. ($CCP_{E2050CLE/MTFR}$-Bio). We further analyzed the independent effects of changing anthropogenic emissions (ΔAnth) under the same 2050 meteorological condition as in Groups 2 and 3.

The benefits of emission reduction were analyzed through the comparison between groups, and will be analyzed in Section 3.3. In order to calculate the CCP benefits of emission reduction for $PM_{2.5}$ under RCP8.5 in 2050 ($\Delta CCP_{CLE/MTFR}$), we compared the differences between CCP from 2015 to 2050 CLE/MTFR meteorological condition under 2015 emissions ($CCP_{E2015\_CLE/E2015\_MTFR}$, defined as the changes from Case 1.1 (2015BASE) to Case 2.4/3.4) and under 2050 CLE/MTFR emissions ($CCP_{E2050CLE}$ and $CCP_{E2050CLE}$, defined in Table 1). Specific calculation method of ΔCCP is listed in Table 2.

For 2050 MTFR emission scenario, we also compared the benefits from ΔCCP_{MTFR} with the reduction potential of $PM_{2.5}$ concentrations due to direct impact of emission reduction (negative $\Delta Anth_{E2050MTFR}$) to calculate the benefit ratio of ΔCCP_{MTFR}: $\Delta CCP_{MTFR} / (\Delta CCP_{MTFR} +$ negative $\Delta Anth_{E2050MTFR}) \times 100\%$.

2.5. Model performance

We compared the simulations with observations from the National Climatic Data Center (NCDC, https://www.ncdc.noaa.gov/data-access/land-based-station-data/) and the China National Environmental Monitoring Centre (http://beijingair.sinaapp.com/). Table S3 lists the model performance statistics for meteorological and chemical variables and benchmarks proposed by Emery et al. (2001) which have been widely accepted in many regional air quality modeling studies (Zhao et al., 2013; Zhao et al., 2019; Zhao et al., 2017; Zhao et al., 2018). The error level of the WRF and CMAQ model is considered to fall within acceptable limits for this study. Detailed description can be found in supplementary materials.

3. Results and discussions

3.1. Future meteorological conditions and biogenic emissions under different anthropogenic emission scenarios

We selected the temperature at 2m (T2), humidity at 2 m (Q2), shortwave radiation (SWDOWN) levels, cloud fraction (CLDFRA) and soil moisture (SMOIS) for analysis, for their large influences on BVOC emission and $PM_{2.5}$ formation (Figs. S3 and S4) (Aydin et al., 2014; Guenther et al., 2012; Li et al., 2013; Liu et al., 2019c; Stanfield et al., 2014; Stathopoulou et al., 2008).

As shown in Fig. 3, compared with in 2015, T2 and Q2 in 2050 CLIM are projected to increase by around 2 K and 1 g kg^{-1} in 2050 in China, respectively, which are consist with IPCC AR5 report (Stocker et al., 2013). Changes in SWDOWN and SMOIS show significant North-South differences, with opposite trends. SWDOWN in the south of the Yangtze River tends to increase, and in the north tends to weaken, except for PRD. T2, Q2, SMOIS and SWDOWN promote BVOC emissions within a certain range (T2 < 290 K, Q2 < 11 g kg^{-1}, SMOIS < 0.3 m^3 m^{-3} and SWDOWN < 190 W m^{-2} in this study based on 13,757 grid data belonging to CHA) in the MEGAN model. Total BVOC emissions are 13.84 Tg C yr^{-1} in 2015 and 18.48 Tg (C) in 2050 CLIM in CHA.

In the simulations of global climate, the use of different emission inventories of 2015, 2050 CLE and 2050 MTFR can generate different meteorological output. The use of different boundary conditions produces local climate responses, although these differences are smaller than those resulting from climate change from 2015 to 2050 under RCP8.5, and may reflect climate variability rather than a significant difference in the climate response to the choice of anthropogenic air pollutant emission inventory. Detailed results are given in Table S4 and Fig. S2.

3.2. Climate change penalties for $PM_{2.5}$ under RCP8.5

In general, future climate change will cause an increase in $PM_{2.5}$ concentrations under the RCP8.5 climate scenarios from 2015 to 2050. Fig. 4 shows the distributions of CCP_{E2015} (a), $CCP_{E2050CLE}$ (b) and

Table 2
Calculation method of ΔCCP from 2015 to 2050 CLE/MTFR meteorological condition under different emissions.

Group	Definition	Calculation method	Notation
CCP from 2015 to 2050 CLE meteorological condition	under 2015 emissions	Case 2.4 – Case 1.1	CCP_{E2015_CLE}
	under 2050CLE emissions	Case 2.1 – Case 2.2	$CCP_{E2050CLE}$
	Benefits from ΔCCP	$CCP_{E2015\_CLE} - CCP_{E2050CLE}$	ΔCCP_{CLE}
CCP from 2015 to 2050 MTFR meteorological condition	under 2015 emissions	Case 3.4 – Case 1.1	CCP_{E2015_MTFR}
	under 2050MTFR emissions	Case 3.1 – Case 3.2	$CCP_{E2050MTFR}$
	Benefits from ΔCCP	$CCP_{E2015\_MTFR} - CCP_{E2050MTFR}$	ΔCCP_{MTFR}

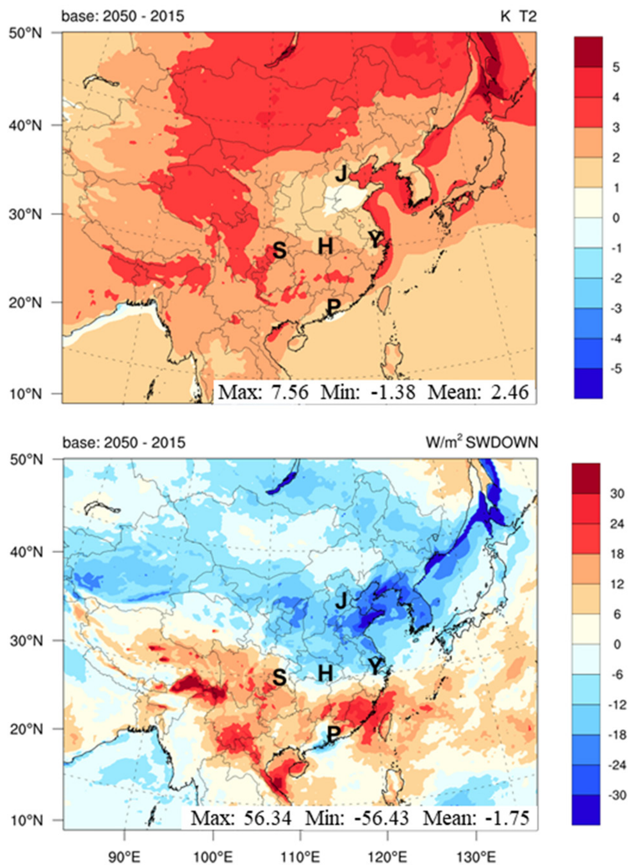

Fig. 3. Changes of major meteorological variables (T2, Q2, SWDOWN and SMOIS) from 2015 to 2050 CLIM under RCP8.5.

$CCP_{E2050MTFR}$ (c) for $PM_{2.5}$ concentrations, respectively. CCP_{E2015} to $PM_{2.5}$ in ECH is 1.43 μg m^{-3}, varying from 0.46 (in PRD) to 3.39 (in HUZ) μg m^{-3} in different typical regions. The increase in inland areas is relatively obvious, such as more than 3 μg m^{-3} in JJJ and HUZ, while in coastal areas is relatively less, such as less than 1 μg m^{-3} in PRD and YRD.

$CCP_{E2050CLE}$ is roughly the same order of magnitude as CCP_{E2015}, except that there is a significant decrease in JJJ and PRD, which may be related to a decrease in T2 and an increase in Q2, respectively. In the 2050CLE case, the increase in $PM_{2.5}$ is even more pronounced than 2050CLIM, with an annual average increase of 5.38 μg m^{-3} in ECH and 2.82 μg m^{-3} in CHA, after considering both CCP and impact of ΔAnth. The contribution of $CCP_{E2050CLE}$ to the total increase of $PM_{2.5}$ concentrations is 23.84% in ECH, whereas such contribution exceeds 50% in HUZ.

After strict emission reduction, $CCP_{E2050MTFR}$ is significantly reduced, with annual average contribution of 0.24 μg m^{-3} in ECH. $CCP_{E2050MTFR}$ has been reduced by 83.40% in ECH compared to CCP_{E2015}, of which the most obvious reductions occur in JJJ and HUZ. Such obvious reduction proves the significance of anthropogenic emission reduction in controlling CCP. The proportion of $PM_{2.5}$ concentration affected by $CCP_{E2050MTFR}$ is 15.43% in ECH (calculated based on the absolute value of the effects) after considering the contributions of $ΔAnth_{E2050MTFR}$ (Fig. S5), and is 8.41% less than proportion of $CCP_{E2050CLE}$.

We further analyzed the impact mechanism of CCP under two emission scenarios (i.e., CLE and MTFR) in 2050, including the effects of meteorological changes on atmospheric processes (i.e., CCP-Met) and the effects of driving biogenic precursors (i.e., CCP-Bio) (Liu et al., 2019b). Because of the unconsidered future changes of plant function and land

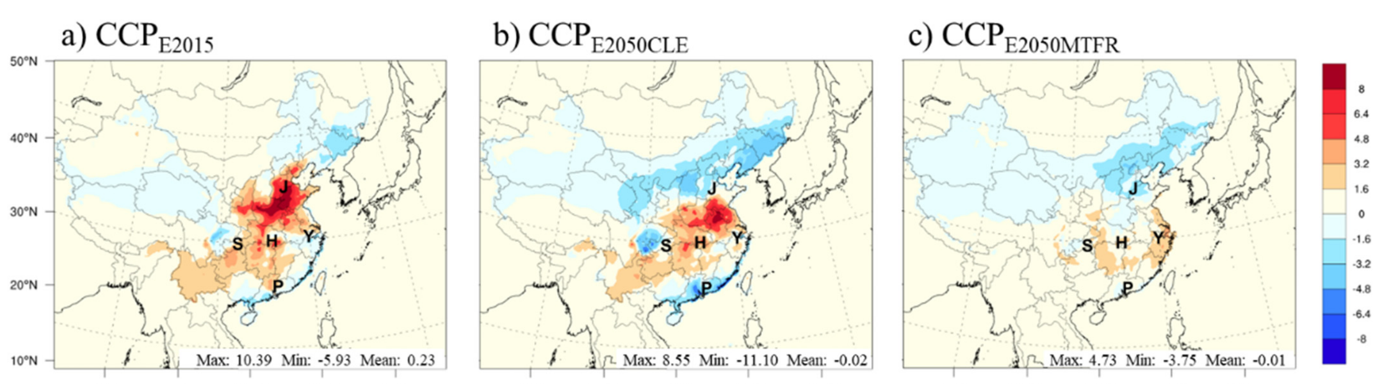

Fig. 4. Climate change penalty for $PM_{2.5}$ based on emissions of 2015 (a), 2050 CLE (b) and 2050 MTFR (c), respectively. (Unit: μg m^{-3}).

cover types, CCP under both emission scenarios are dominated by CCP-Met. The proportion of CCP-Met is around 60% under both 2050CLE and MTFR emission scenarios. The proportion of CCP-Met in five typical regions is higher than domain average, with an average of 85%. Fig. 5a) and b) shows the changes of $PM_{2.5}$ concentrations by CCP-Met under 2050CLE and MTFR emission scenarios. The difference of regional distribution of CCP-Met is consistent with that of CCP. Although judging from the range of change, $CCP_{E2050MTFR}$-Met is weaker than $CCP_{E2050CLE}$-Met, considering the absolute amount of change, CCP-Met under 2050CLE and MTFR emission scenarios is of the same order of magnitude, with an average difference of only 0.05 μg m^{-3} in CHA, indicating that it is difficult to control the concentration of $PM_{2.5}$ from this path after emissions reduction.

Under each case in 2050, changes in BVOC emissions (i.e., CCP-Bio) have a positive impact on $PM_{2.5}$, but the average annual impact is within 1 μg m^{-3}. It is worth noting that the BVOC emissions under the 2050 MTFR meteorological condition are basically the same as the 2050 CLE in the order of magnitude, and even higher in ECH and CHA, but the impact of $CCP_{E2050MTFR}$-Bio on $PM_{2.5}$ is lower than $CCP_{E2050CLE}$-Bio (about three quarters of the level), as shown in Fig. 5c) and d). After anthropogenic emission reduction, the contribution of CCP-Bio can be reduced by 26.63% in ECH. This suggests that the impact of BVOC on secondary pollutants is subject to anthropogenic emissions because BVOC emissions are generally saturated. Therefore, the control of anthropogenic emissions will also reduce the contribution of BVOC to secondary pollutants, which is corroborated by our previous research (Liu et al., 2019b).

Table 3
The benefits of emission reduction on $PM_{2.5}$ concentrations under RCP8.5 in 2050.

Scenario	Benefits from	JJJ	YRD	PRD	SCH	HUZ	ECH	CHA
2050 CLE	ΔAnth	−3.79	−8.80	−7.01	−6.65	−5.83	−4.10	−2.20
	ΔCCP	2.19	0.12	0.62	0.70	2.35	1.22	0.68
2050 MTFR	ΔAnth	19.74	18.25	8.29	13.63	24.19	12.71	6.92
	ΔCCP	4.46	3.44	0.13	0.86	3.10	2.08	1.03
	Ratio of ΔCCP (%)	18.43	15.87	1.58	5.92	11.37	14.07	12.90

Benefits from ΔCCP are calculated as the ΔCCP under 2015 emissions ($CCP_{E2015\_CLE/MTFR}$) minus under 2050 CLE/MTFR emissions ($CCP_{E2050CLE/MTFR}$) (Unit: μg m^{-3}). Negative values represent increased concentration.
JJJ: Beijing-Tianjin-Hebei region; YRD: The Yangtze River Delta; PRD: The Pearl River Delta; SCH: The Sichuan Basin; HUZ: Central China; ECH: Eastern China that includes the above five typical regions; CHA: Mainland China.

Considering that BVOC emissions are concentrated in summer (June to August) and contribute more to organic components in $PM_{2.5}$, we further analyzed the impact of changes in BVOC emissions on SOA concentrations during summer in Fig. S6 and Table S5. The contribution ratios of biogenic emissions to SOA are about 47.17% and 18.55% under the 2050 CLE and 2050 MTFR emission scenarios, respectively, with obvious regional differences. Taken together, controlling anthropogenic emissions can help reduce the impact of BVOC emissions on SOA.

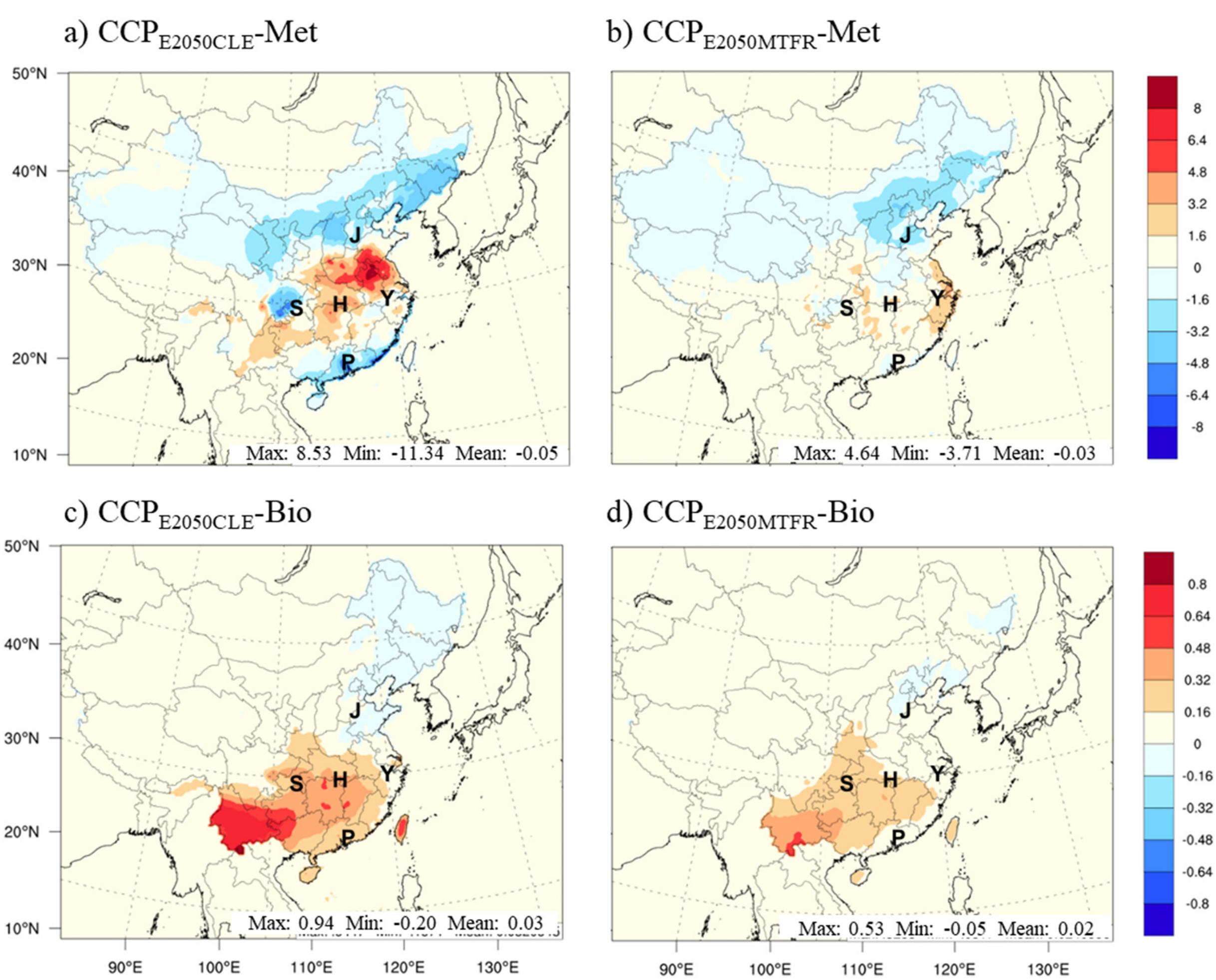

Fig. 5. Distributions of annual average concentrations of $PM_{2.5}$ contributed by changed meteorology (upper) or BVOC (bottom) emissions under the 2050 CLE (left) and MTFR (right) emission scenarios. (Unit: μg m^{-3}).

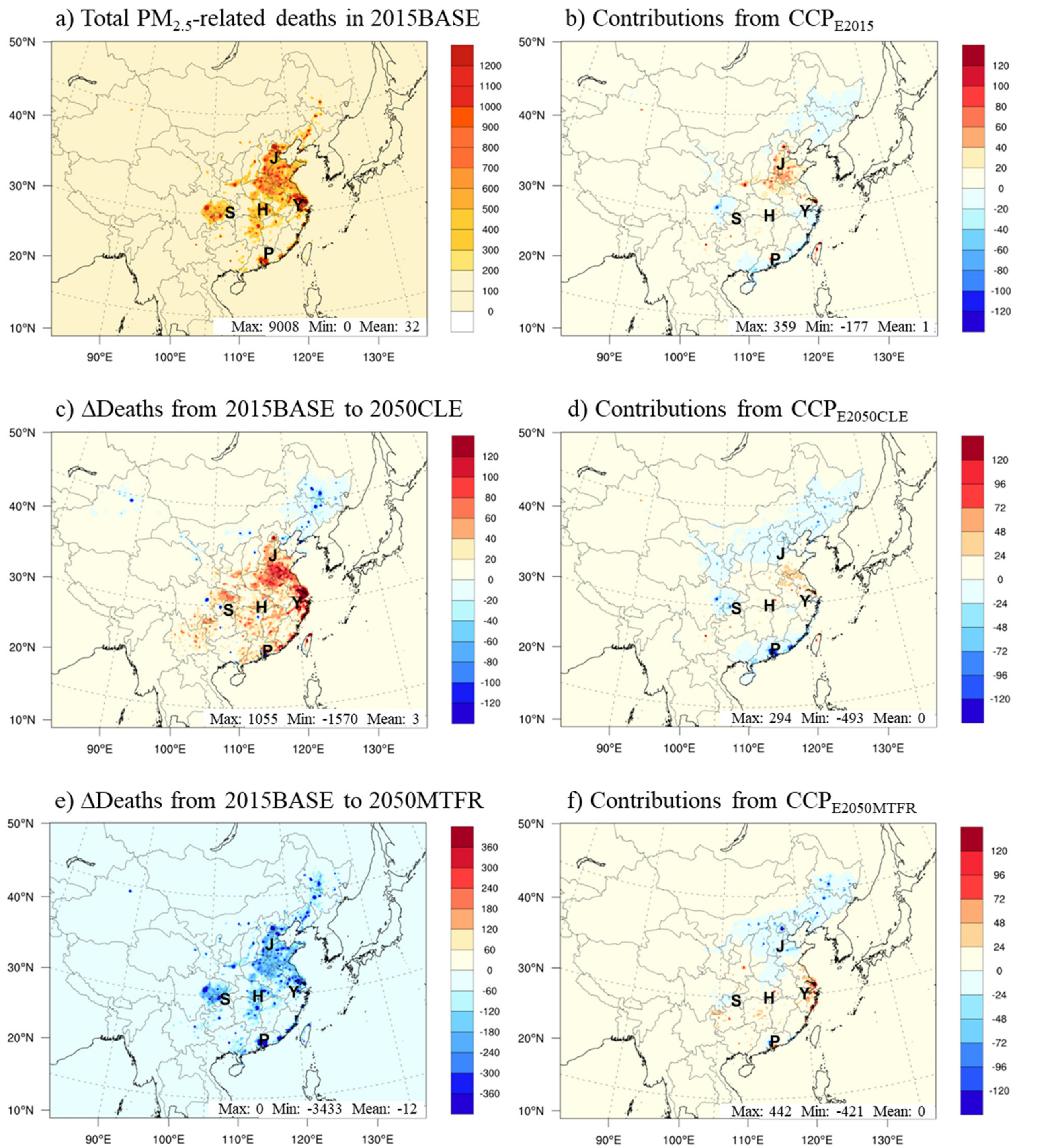

Fig. 6. Distributions of total $PM_{2.5}$-related deaths in 2015BASE (a), changes from 2015BASE to 2050CLE (c) and 2050MTFR (e), and contributions of climate change penalties using different emissions (b, d, f).

3.3. Benefits from emission reduction in reducing the climate change penalties

Although the CCP still exists under the MTFR emission scenario of strict emission reduction, it is much smaller than the CCP under higher-emission scenarios. We analyzed the effects of regulating anthropogenic emissions on the CCP. Table S6 lists the detailed concentrations of $PM_{2.5}$ in typical regions for each case.

Considering the climate change from 2015 to 2050 CLE, the use of 2050 CLE emission inventory has a higher enhancement to $PM_{2.5}$ concentrations than using 2015 emissions. Using 2050 CLE emissions produced a 0.68 μg m^{-3} reduction (ΔCCP_{CLE}) on $PM_{2.5}$ in CHA compared to the CCP with 2015 emissions. After reducing emissions (MTFR emission scenario), the impact of CCP on $PM_{2.5}$ concentrations is reduced by 2.08 μg m^{-3} (ΔCCP_{MTFR}) from 2015 to 2050 MTFR compared to using 2015 emissions. The reduction of anthropogenic emissions can reduce $PM_{2.5}$ concentrations by 12.71 μg m^{-3} in ECH. 14.07% of the benefits of emission reduction on $PM_{2.5}$ is achieved by reducing the impact of CCP in ECH. Table 3 lists the specific results for typical regions. For most regions, benefits of ΔCCP_{MTFR} are significantly improved compared with ΔCCP_{CLE}, except for PRD. This is because Q2 of 2050 CLE increases significantly in PRD, making ΔCCP_{CLE} more conducive to the reduction of $PM_{2.5}$ concentrations. In addition, the fluctuation of regional meteorological fields is also a possible major reason.

The CCP for $PM_{2.5}$ will increase $PM_{2.5}$-mortality. Fig. S7 shows the changes in total $PM_{2.5}$-related deaths in typical regions under different emission scenarios in 2050 compared to 2015BASE, to quantifying the impact of emissions on health burden for specific region. Total $PM_{2.5}$-related deaths is estimated to be 1.32 million per year in China in 2015BASE, and may increase by 35,000 in 2050CLIM on average for CHA. Fig. 6(a) and (b) shows the distributions of total $PM_{2.5}$-related deaths in 2015 and contributions of CCP_{E2015} using 2015 emissions. The $PM_{2.5}$-related deaths in five typical regions all tend to increase, but in PRD and SCH have grown by less than 1000. The number of $PM_{2.5}$-related deaths caused by CCP_{E2015} increased the most in JJJ, reaching 8600.

Total $PM_{2.5}$-related deaths is 116,270 more in the 2050CLE case compared to 2015BASE. Fig. 6(c) shows the distributions of changes of total $PM_{2.5}$-related deaths between 2050CLE and 2015BASE. In the 2050CLE case, YRD has the largest increase in $PM_{2.5}$ concentrations, which is related to its significantly increased NO_x and SO_2 emissions, leading to an increase of 12.29% in $PM_{2.5}$-mortality compared to 2015BASE. The contribution of $CCP_{E2050CLE}$ to $PM_{2.5}$-mortality is about 20%, as shown in Fig. 6(d). Since the promotion or suppression affection varies by regions, it will be offset when summed. Overall, compared with CCP_{E2015_CLE}, $CCP_{E2050CLE}$ on $PM_{2.5}$-mortality may be reduced, but it is still on the same order of magnitude.

The amount of changes in $PM_{2.5}$ concentrations directly affects the $PM_{2.5}$-mortality. Controlling emissions can effectively achieve $PM_{2.5}$ health benefits. Total $PM_{2.5}$-related deaths can be reduced by 36.90% under the 2050MTFR case compared to 2015BASE. In JJJ and HUZ, the number of $PM_{2.5}$-mortality decrease the most, but considering the difference in base numbers, the reduction in PRD is the largest at 47.86% under the 2050MTFR case. Existed $CCP_{E2050MTFR}$ will cause an additional 17,360 deaths in ECH. Fig. 6(e) and (f) shows the changes in total $PM_{2.5}$-related deaths compared to 2015BASE under the 2050 MTFR emission scenario and the impact of $CCP_{E2050MTFR}$, respectively. Compared with CCP_{E2015_MTFR}, $CCP_{E2050MTFR}$ on $PM_{2.5}$-mortality using low-emission inventories can reduce $PM_{2.5}$-related deaths by 45,930, which is 24.14% of the total health benefits.

4. Summary and conclusion

This study estimated future climate change penalties and associated $PM_{2.5}$-mortality under different anthropogenic emissions in China using the WRF, MEGAN, CMAQ and BenMAP models. We find an annual average contribution of the climate change penalty to $PM_{2.5}$ under RCP8.5 in ECH of 1.43 μg m^{-3} if future anthropogenic emissions are kept the same level as 2015, which may lead to 35,000 more deaths related to $PM_{2.5}$. This climate change penalty can play an important role in determining future $PM_{2.5}$ concentrations and related deaths, and deserves our attention to find ways to reduce it.

The climate change penalty on $PM_{2.5}$ concentrations estimated with the 2050CLE emissions is roughly similar to the 2015 emissions. However, it can be significantly reduced to 0.24 μg m^{-3} (by 83.40%) in ECH after strict emission reduction (using the 2050 MTFR emissions), suggesting significant benefits of emission control in reducing the climate change penalty. Such benefits account for 14% of the total air quality benefits and 24.14% of the total health benefits associated with MTFR emission scenarios. The control of anthropogenic emissions can effectively reduce the climate change penalty on $PM_{2.5}$ and its associated premature deaths, though the climate change penalty still exists even under the MTFR.

After dividing the impact of climate change penalty into the effects of meteorological changes on atmospheric processes and the effects of driving biogenic emissions, we found that the former mechanism dominates the climate change penalties. But the latter mechanism is more sensitive to anthropogenic emission reductions, because the emissions of BVOCs are usually saturated. After anthropogenic emission reduction, the contribution of climate change penalty to $PM_{2.5}$ concentrations by BVOCs can be reduced by 26.63% in ECH.

Further, global warming and climate changes suffer large concerns especially after the U.S. withdrawal from the Paris Agreement in 2019. Our study demonstrated that strengthened controls on anthropogenic emissions is the key to ensure air quality targets and protect human health even under the challenge of a pessimistic future global warming scenario, for its effectiveness in reducing the climate change penalty driving by the continual increases of GHGs.

CRediT authorship contribution statement

Song Liu: Writing- Original draft preparation, Plots, Methodology, Validation, Model running.

Jia Xing: Data Curation, Supervision, Conceptualization, Writing-Reviewing and Editing.

Daniel M. Westervelt: Model running, Writing- Reviewing and Editing.

Shuchang Liu: Methodology, Model running.

Dian Ding: Methodology, Model running.

Arlene M. Fiore: Data Curation, Writing- Reviewing and Editing.

Patrick L Kinney: Data Curation, Writing- Reviewing and Editing.

Yuqiang Zhang: Writing- Reviewing and Editing.

Mike Z. He: Data Curation.

Hongliang Zhang: Model input data preparing.

Shovan K. Sahu: Writing- Reviewing and Editing.

Fenfen Zhang: Methodology.

Bin Zhao: Writing- Reviewing and Editing.

Shuxiao Wang: Supervision, Conceptualization, Writing- Reviewing and Editing.

Declaration of competing interest

The authors wish to confirm that there are no known conflicts of interest associated with this publication and there has been no significant financial support for this work that could have influenced its outcome.

Acknowledgements

This work was supported in part by National Key Research and Development Program of China (2018YFC0213502 & 2018YFC0213506), and National Natural Science Foundation of China (21625701, 4190070530 & 51861135102). This work was completed on the “Explorer 100” cluster system of Tsinghua National Laboratory for Information Science and Technology.

Appendix A. Supplementary data

Supplementary data to this article can be found online at https://doi.org/10.1016/j.scitotenv.2020.144338.

References

Appel, K., Pouliot, G., Simon, H., Sarwar, G., Pye, H., Napelenok, S., et al., 2013. Evaluation of dust and trace metal estimates from the Community Multiscale Air Quality (CMAQ) model version 5.0. Geosci. Model Dev. 6, 883–899.

Appel, K.W., Napelenok, S., Hogrefe, C., Pouliot, G., Foley, K.M., Roselle, S.J., et al., 2018. Overview and evaluation of the community multiscale air quality (CMAQ) modeling system version 5.2. In: Mensink, C., Kallos, G. (Eds.), Air Pollution Modeling and its Application XXV. ITM 2016. Springer Proceedings in Complexity. Springer, Cham, pp. 69–73.

Aydin, Y.M., Yaman, B., Koca, H., Dasdemir, O., Kara, M., Altiok, H., et al., 2014. Biogenic volatile organic compound (BVOC) emissions from forested areas in Turkey: determination of specific emission rates for thirty-one tree species. Sci. Total Environ. 490, 239–253.

Burnett, R., Chen, H., Szyszkowicz, M., Fann, N., Hubbell, B., Pope, C.A., et al., 2018. Global estimates of mortality associated with long-term exposure to outdoor fine particulate matter. Proc. Natl. Acad. Sci. 115, 9592–9597.
Byun, D., 1999. Science Algorithms of the EPA Models-3 Community Multiscale Air Quality (CMAQ) Modeling System. EPA/600/R-99/030.
Cohen, A.J., Brauer, M., Burnett, R., Anderson, H.R., Frostad, J., Estep, K., et al., 2017. Estimates and 25-year trends of the global burden of disease attributable to ambient air pollution: an analysis of data from the Global Burden of Diseases Study 2015. Lancet 389, 1907–1918.
Ding, D., Xing, J., Wang, S., Liu, K., Hao, J., 2019. Estimated contributions of emissions controls, meteorological factors, population growth, and changes in baseline mortality to reductions in ambient PM2.5 and PM2.5-related mortality in China, 2013–2017. Environ. Health Perspect. 127 (6) 67009–67009.
Donner, L.J., Wyman, B.L., Hemler, R.S., Horowitz, L.W., Ming, Y., Zhao, M., et al., 2011. The dynamical core, physical parameterizations, and basic simulation characteristics of the atmospheric component AM3 of the GFDL global coupled model CM3. J. Clim. 24, 3484–3519.
Emery, C., Tai, E., Yarwood, G., 2001. Enhanced Meteorological Modeling and Performance Evaluation for Two Texas Ozone Episodes. Prepared for the Texas Natural Resource Conservation Commission, by ENVIRON International Corporation.
Fann, N., Fulcher, C.M., Baker, K., 2013. The recent and future health burden of air pollution apportioned across US sectors. Environ. Sci. Technol. 47, 3580–3589.
Fu, T.-M., Tian, H., 2019. Climate change penalty to ozone air quality: review of current understandings and knowledge gaps. Curr. Pollution Rep. 5 (3), 1–13.
Gao, D., Xie, M., Chen, X., Wang, T., Liu, Q., 2019. Modeling the effects of climate change on surface ozone during summer in the Yangtze River Delta region, China. Int. J. Environ. Res. Public Health 16, 1528.
Guenther, A., Jiang, X., Heald, C., Sakulyanontvittaya, T., Duhl, T., Emmons, L., et al., 2012. The Model of Emissions of Gases and Aerosols From Nature Version 2.1 (MEGAN2. 1): An Extended and Updated Framework for Modeling Biogenic Emissions.
Heald, C., Henze, D., Horowitz, L., Feddema, J., Lamarque, J.F., Guenther, A., et al., 2008. Predicted change in global secondary organic aerosol concentrations in response to future climate, emissions, and land use change. Journal of Geophysical Research: Atmospheres 113.
Hu, J., Wang, P., Ying, Q., Zhang, H., Chen, J., Ge, X., et al., 2017. Modeling biogenic and anthropogenic secondary organic aerosol in China. Atmos. Chem. Phys. 17, 77–92.
Jacob, D.J., Winner, D.A., 2009. Effect of climate change on air quality. Atmos. Environ. 43, 51–63.
Jiang, H., Liao, H., Pye, H., Wu, S., Mickley, L., Seinfeld, J., et al., 2013. Projected effect of 2000-2050 changes in climate and emissions on aerosol levels in China and associated transboundary transport. Atmos. Chem. Phys. 13, 7937–7960.
Jiang, X., Yang, Z.L., Liao, H., Wiedinmyer, C., 2010. Sensitivity of biogenic secondary organic aerosols to future climate change at regional scales: an online coupled simulation. Atmos. Environ. 44, 4891–4907.
Kan, H., Chen, B., 2004. Particulate air pollution in urban areas of Shanghai, China: health-based economic assessment. Sci. Total Environ. 322, 71–79.
Leung, D.M., Tai, A.P., Shen, L., Moch, J.M., van Donkelaar, A., Mickley, L.J., 2017. Impacts of 2000-2050 climate change on fine particulate matter (PM 2.5) air quality in China based on statistical projections using an ensemble of global climate models. AGUFM 2017, A43L-06.
Levy, H., Horowitz, L.W., Schwarzkopf, M.D., Ming, Y., Golaz, J.C., Naik, V., et al., 2013. The roles of aerosol direct and indirect effects in past and future climate change. Journal of Geophysical Research: Atmospheres 118, 4521–4532.
Li, G., 2019. Report on the Completion of Environmental Conditions and Environmental Protection Targets for 2018. (in Chinese).
Li, J., Wang, G., Cao, J., Wang, X., Zhang, R., 2013. Observation of biogenic secondary organic aerosols in the atmosphere of a mountain site in central China: temperature and relative humidity effects. Atmos. Chem. Phys. 13, 11535–11549.
Liao, H., Chen, W.T., Seinfeld, J.H., 2006. Role of climate change in global predictions of future tropospheric ozone and aerosols. Journal of Geophysical Research: Atmospheres 111.
Liu, R., Liao, H., Chang, W., 2017. al. e. Impact of climate change on aerosol concentrations in eastern China based on Atmospheric Chemistry and Climate Model Intercomparison Project (ACCMIP) datasets. Chin. J. Atmos. Sci. 41, 739–751.
Liu, S., Xing, J., Wang, S., Ding, D., Hao, J., 2019a. Revealing the impacts of transboundary pollution on PM2.5-related deaths in China. Environ. Int. 105323, 134.
Liu, S., Xing, J., Zhang, H., Ding, D., Zhang, F., Zhao, B., et al., 2019b. Climate-driven trends of biogenic volatile organic compound emissions and their impacts on summertime ozone and secondary organic aerosol in China in the 2050s. Atmos. Environ. 218, 117020.
Liu, S., Xing, J., Zhao, B., Wang, J., Wang, S., Zhang, X., et al., 2019c. Understanding of aerosol–climate interactions in China: aerosol impacts on solar radiation, temperature, cloud, and precipitation and its changes under future climate and emission scenarios. Current Pollution Reports 1–16.
Liu, Y., Xing, J., Wang, S., Fu, X., Zheng, H., 2018. Source-specific speciation profiles of PM 2.5 for heavy metals and their anthropogenic emissions in China. Environ. Pollut. 239, 544–553.
Otte, T., Pleim, J., 2010. The meteorology-chemistry interface processor (MCIP) for the CMAQ modeling system: updates through MCIPv3. 4.1. Geoscientific model. Development 3, 243.
Sarwar, G., Luecken, D., Yarwood, G., Whitten, G.Z., Carter, W.P.L., 2008. Impact of an updated carbon bond mechanism on predictions from the CMAQ modeling system: preliminary assessment. Journal of Applied Meteorology & Climatology 47, 3–14.
Schulzweida, U., Kornblueh, L., Quast, R., 2006. CDO user's guide. Climate data operators, Version 1, 205–209.
Stanfield, R.E., Dong, X., Xi, B., Kennedy, A., Del Genio, A.D., Minnis, P., et al., 2014. Assessment of NASA GISS CMIP5 and post-CMIP5 simulated clouds and TOA radiation budgets using satellite observations. Part I: cloud fraction and properties. J. Clim. 27, 4189–4208.
Stathopoulou, E., Mihalakakou, G., Santamouris, M., Bagiorgas, H., 2008. On the impact of temperature on tropospheric ozone concentration levels in urban environments. Journal of Earth System Science 117, 227–236.
Stocker, T.F., Qin, D., Plattner, G., Tignor, M., Allen, S., Boschung, J., et al., 2013. Climate Change 2013: The Physical Science Basis. Intergovernmental Panel on Climate Change, Working Group I Contribution to the IPCC Fifth Assessment Report (AR5). New York.
Stohl, A., Aamaas, B., Amann, M., Baker, L., Bellouin, N., Berntsen, T.K., et al., 2015. Evaluating the climate and air quality impacts of short-lived pollutants. Atmos. Chem. Phys. 15, 10529–10566.
Streets, D.G., Fu, J.S., Jang, C.J., Hao, J., He, K., Tang, X., et al., 2007. Air quality during the 2008 Beijing Olympic Games. Atmos. Environ. 41, 480–492.
Su, X., Teng, F., 2019. The effects of U.S. withdrawal from the Paris Agreementon global GHGs emissions. Clim. Chang. Res. 15 (01), 74–83.
The State Council of the People's Republic of China, 2013. Air Pollution Prevention and Control Action Plan. (in Chinese).
Voorhees, A.S., Wang, J., Wang, C., Zhao, B., Wang, S., Kan, H., 2014. Public health benefits of reducing air pollution in Shanghai: a proof-of-concept methodology with application to BenMAP. Sci. Total Environ. 485, 396–405.
Wang, L., Xu, J., Yang, J., Zhao, X., Wei, W., Cheng, D., et al., 2012. Understanding haze pollution over the southern Hebei area of China using the CMAQ model. Atmos. Environ. 56, 69–79.
Westervelt, D., Ma, C., He, M., Fiore, A., Kinney, P., Kioumourtzoglou, M., et al., 2019. Mid-21st century ozone air quality and health burden in China under emissions scenarios and climate change. Environ. Res. Lett. 14, 074030.
Westervelt, D.M., Horowitz, L.W., Naik, V., Tai, A.P.K., Fiore, A.M., Mauzerall, D.L., et al., 2016. Quantifying PM2.5-meteorology sensitivities in a global climate model. Atmos. Environ. 142, 43–56.
Xie, M., Shu, L., Wang, T.-J., Liu, Q., Gao, D., Li, S., et al., 2017. Natural emissions under future climate condition and their effects on surface ozone in the Yangtze River Delta region, China. Atmos. Environ. 150, 162–180.
Yin, C., Wang, T., Zhuang, B., Deng, X., Deng, T., Wang, N., 2015. China's future secondary organic aerosol prediction under RCP scenario. The 32nd Annual Meeting of the Chinese Meteorological Society, Tianjin, China, p. 1.
Zhang, Y., Liao, H., Ding, X., Jo, D., Li, K., 2018. Implications of RCP emissions on future concentration and direct radiative forcing of secondary organic aerosol over China. Sci. Total Environ. 640, 1187–1204.
Zhao, B., Wang, S., Wang, J., Fu, J.S., Liu, T., Xu, J., et al., 2013. Impact of national NOx and SO2 control policies on particulate matter pollution in China. Atmos. Environ. 77, 453–463.
Zhao, B., Wu, W., Wang, S., Xing, J., Chang, X., Liou, K.-N., et al., 2017. A modeling study of the nonlinear response of fine particles to air pollutant emissions in the Beijing-Tianjin-Hebei region. Atmos. Chem. Phys. 17 (19), 1–35.
Zhao, B., Zheng, H., Wang, S., Smith, K.R., Lu, X., Aunan, K., et al., 2018. Change in household fuels dominates the decrease in PM2. 5 exposure and premature mortality in China in 2005–2015. Proc. Natl. Acad. Sci. 115, 12401–12406.
Zhao, B., Wang, T., Jiang, Z., Gu, Y., Liou, K.-N., Kalandiyur, N., et al., 2019. Air quality and health co-benefits of different deep decarbonization pathways in California. Environ. Sci. Technol. 53 (12).
Zheng, H., Zhao, B., Wang, S., Wang, T., Ding, D., Chang, X., et al., 2019. Transition in source contributions of PM 2.5 exposure and associated premature mortality in China during 2005–2015. Environ. Int. 132.